



A Hybrid Energy Storage System for an Electric Vehicle and Its Effectiveness Validation

Chunhua Zheng¹ · Yafei Wang¹ · Zhongxu Liu¹ · Tianfu Sun¹ · Namwook Kim² · Jongryeol Jeong³ · Suk Won Cha³

Received: 16 June 2020 / Revised: 6 December 2020 / Accepted: 11 December 2020 / Published online: 22 March 2021
© Korean Society for Precision Engineering 2021

Abstract

A hybrid energy storage system (HESS), which consists of a battery and a supercapacitor, presents good performances on both the power density and the energy density when applying to electric vehicles. In this research, an HESS is designed targeting at a commercialized EV model and a driving condition-adaptive rule-based energy management strategy (EMS) is proposed for the HESS, which takes into account the superiority achievement of each ESS and also the protection to each ESS. The effectiveness of the HESS plus the EMS compared to the single battery case is validated by both the computer simulation and the semi-physical rapid control prototype (RCP) test bench. An electric loading equipment is adopted in the RCP experiment validation for simulating the vehicle driving cycle instead of the traditional combination of a motor and a dynamometer. Both validation results show that compared to the single battery case, the working status of the battery is stabilized by the addition of the supercapacitor in the HESS case during both the propelling and regeneration modes and the battery energy is also saved. A dynamic degradation model for the battery is adopted in order to evaluate the life cycle cost of the HESS. Results show that the HESS plus the EMS has the effect of prolonging the battery lifetime and the HESS is economically effective compared to the single battery case.

Keywords Hybrid energy storage system · Electric vehicle · Energy management strategy · Rapid control prototype · Lifetime prolonging · Energy saving · Life cycle cost

1 Introduction

A single energy storage system (ESS) is commonly used in electric vehicles (EVs) currently. The ESS should satisfy both the power and energy density requirements as EVs should be able to cover a complicated driving cycle, including starting, acceleration, cruising, and deceleration modes, and meet a long driving mileage per charging. However, each single ESS has some inherent demerits. For example, batteries present a much lower power density, a shorter

cycle life, a much longer charging time, a worse starting performance at low temperature compared to supercapacitors, whereas supercapacitors provide a much lower energy density compared to batteries. Currently, there is no such a single ESS which meets the power density and the energy density requirements of EVs at the same time. A hybrid ESS (HESS), in which a battery is the main ESS and a supercapacitor is the auxiliary ESS, can figure out the problems by combining the energy density superiority of the battery and the power density superiority of the supercapacitor. Because of the use of two ESSs, the HESS should be accompanied by an energy management strategy (EMS) to distribute the totally required power between the two ESSs appropriately, otherwise the energy may be wasted.

Regarding the EMS of the HESS for EVs, there have been two major types of EMSs, which are the heuristic concept-based EMS [1–10] and the optimal control theory-based EMS [3, 9, 11] respectively. The former EMS is established by a number of rules or fuzzy logics, which are based on expert knowledge. This type of EMS is simple and its logic relationship is explicit, thus it is convenient for the

✉ Suk Won Cha
swcha@snu.ac.kr

¹ Shenzhen Institutes of Advanced Technology, Chinese Academy of Sciences, 1068 Xueyuan Avenue, Shenzhen University Town, Shenzhen 518055, China

² Department of Mechanical Engineering, Hanyang University, Ansan, Gyeonggi-do 15588, South Korea

³ Department of Mechanical Engineering, Seoul National University, 1 Gwanak-ro, Gwanak-gu, Seoul 08826, South Korea

implementation. Research [1] proposed an EMS which is based on simple rules and takes advantage of the high power density of the supercapacitor and prevents an overstress on the battery. Research [2] presented a novel rule-based EMS by considering two objectives which are improving the vehicle's efficiency and reducing peak battery currents to increase the battery life. Several heuristic concept-based EMSs were proposed and compared for bus applications in research [3] including a rule-based EMS and a fuzzy logic-based EMS, and comparison results showed that the rule-based and the fuzzy logic-based EMSs reduce more than 50% of the battery capacity loss along the China Bus Driving Cycle compared to the single battery configuration. In research [4], a rule based EMS was developed aiming at exploiting the supercapacitor characteristics and increasing the battery lifetime and the system efficiency, and the effectiveness of the proposed EMS was validated by experiments and results showed that the integration of the supercapacitor enables the battery to share the low frequency load current, which would be very helpful to increase the battery lifetime. In addition to above EMSs, there is also a totally different concept of rule-based EMS named the frequency-based strategy [7–10], the main idea of which is to allocate the low and high frequency contents of the demanded power into the battery and the supercapacitor respectively based on Wavelet Transform.

In spite of the aforementioned advantages, the heuristic concept-based EMS is difficult to achieve the theoretically optimal results on the energy management between the battery and the supercapacitor. Thus, the optimal control theory-based EMS is developed later for HESSs. This type of EMS is also widely used to the engine/battery hybrid vehicles [12, 13], which adopts either the global optimization theory including Dynamic Programming (DP) and the instantaneous optimization theory including Pontryagin's Minimum Principle (PMP). An optimal EMS was proposed based on the PMP in research [9], the objective of which is to minimize the electricity usage of the EV and meanwhile to maximize the battery lifetime, and simulation results showed that the proposed EMS saves electricity and has the effect of prolonging the battery lifetime compared to a rule-based EMS and the single ESS case. Research [11] presented a DP algorithm-based EMS including a simplified battery ageing model in the formulation, and simulation results showed that the root mean square value of the battery current is reduced by 10% compared to a rule-based EMS whilst the battery peak current value is also decreased by 45% compared to the same rule-based EMS, which is helpful for prolonging the battery lifetime. The optimal control theory-based EMS guarantees the theoretically optimal results on the energy management, however it cannot be used to the real controllers for the global optimization theory case because of the excessively long calculation time, the backward calculation

process, and the whole driving cycle information-in-advance requirement. For the instantaneous optimization theory case, the difficulty lies in the heavy computational burden for real-time applications and the determination of the control parameters, which depend on the driving condition.

Each type of EMS mentioned above has its own merits and demerits. Thus, some researchers [14–17] have developed new EMSs for HESSs by combing the heuristic concept and the optimal control theory including Simulated Annealing (SA), Particle Swarm Optimization (PSO), and Genetic Algorithm (GA). Research [14] proposed a near-optimal EMS, in which control rules were extracted from DP results, and proved that a well-tuned rule-based EMS presents a good performance when compared to DP approach. Research [15] proposed a rule-based EMS in which SA was introduced to optimize the reference supercapacitor SOC and the battery power, so that the most suitable mode of the multi-mode HESS could be selected and the global energy management optimization of the HESS could also be well realized. A fuzzy logic-based EMS was presented in research [17], in which GA was adopted to optimize lower and upper limits of membership functions aiming to maximize the driving range and performance of the EV.

Regarding the effectiveness validation of the HESS plus the EMS, it is generally a three-step process, which consists of the computer simulation, the semi-physical experiment, and the real vehicle test. Because of the relatively low cost and short time required, the computer simulation technique is adopted by most researchers for the first validation step. However, the reliability is relatively low due to the ideal simulation environment and the validation is also influenced by the simulation model precision. The semi-physical experiment validation is the next step to the computer simulation validation, in which a part of components are switched to real components, so that the reliability can be improved compared to the computer simulation validation and the time and cost can be saved compared to the real vehicle test. In the rapid control prototype (RCP) semi-physical experiment, the controller is virtual and the control objects are real. In research [4], a rule-based EMS was proposed and validated by the RCP experiment based on a dSPACE-based MicroAutoBox (DS1401). Research [15] presented an SA-adaptive mode switch strategy, by which the global energy management optimization of the multi-mode HESS can be well realized, and the effectiveness of the strategy was proved by the RCP experiment using a microcontroller MSP430f5438a and two control boxes. A similar validation work was also carried out in another research [18]. In research [19], the proposed SA-based EMS was tested by the RCP experiment based on the Compact RIO real-time controller. Similarly, in their further research [20], the proposed PSO-based EMS was implemented using the Compact RIO real-time controller for RCP experiment validation. In

research [21], a fuzzy logic-based EMS was implemented using the xPC Target for the RCP experiment validation. In their further research [22], the rule-based strategy, DP algorithm, and real-time reinforcement learning algorithm were systematically compared, and the performance of the control strategies was tested by the RCP experiment based on the xPC Target.

In this research, an HESS is designed targeting at a commercialized EV model, i.e. BMW i3. In spite of the merits of other types of EMS mentioned above, a rule-based EMS is developed for the designed HESS considering that this type of EMS can be easily implemented in a real vehicle. The developed EMS is driving condition-adaptive and considers the superiority achievement of each ESS and the protection to each ESS. There are several control parameters defined in the EMS, which are dependent on the driving condition. The effectiveness of the designed EHSS plus the developed EMS compared to the single battery case is validated by both the computer simulation and the semi-physical test bench, which is constructed based on the RCP using the dSPACE. In the RCP validation, an electric loading equipment is adopted for simulating the vehicle driving cycle instead of the traditional combination of a motor and a dynamometer. This is beneficial for increasing the precision of the driving cycle modeling due to the simple working principle and high controllability of the electric loading equipment and also helpful for reducing the validation risk and cost. The effectiveness of the HESS plus the EMS compared to the single battery case mainly includes the battery lifetime prolonging, the battery electricity saving, and the life cycle cost down in this research. The economic effectiveness of the HESS is proved by adopting a dynamic battery degradation model and comparing the life cycle cost between the HESS and the single battery cases.

2 The Vehicle Model and the HESS Design

The powertrain configuration of the EV with the HESS studied in this research is illustrated in Fig. 1. Regarding the HESS topology, the passive, active, and semi-active topologies were proposed and compared to each other in the research [23–25]. It can be concluded as follows: the power density superiority of the supercapacitor is limited in the passive configuration, in which there is no bidirectional DC/DC converter and thus the energy transfer in the battery and in the supercapacitor is passively controlled; the performance of the active configuration can be the best, in which the energy transfer in the battery and in the supercapacitor is controlled by two bidirectional DC/DC converters respectively, however, this configuration increases the cost and the difficulty in control; the semi-active configuration can be the most effective one considering both the cost and controllability, in which the energy in the supercapacitor

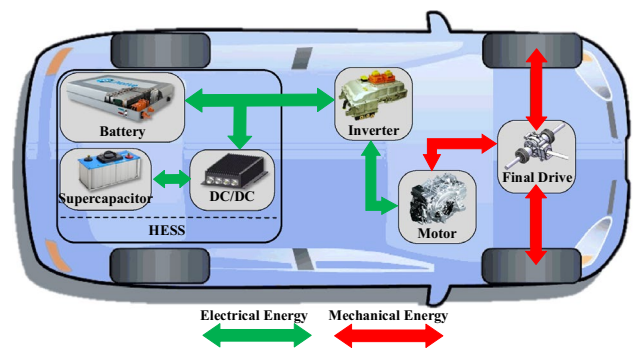


Fig. 1 Powertrain configuration of an EV with an HESS

Table 1 Vehicle parameters of the BMW i3

Parameter	Value
Vehicle total mass (kg)	1443
Wheel base (mm)	2570
Vehicle size (mm)	4006 × 1775 × 1600
Max speed of vehicle (km/h)	150
Transmission gear ratio	9.67:1
Propulsion mode	RR

is controlled by a bidirectional DC/DC converter while that in the battery is controlled passively. Thus, the semi-active configuration is adopted in this research for the HESS topology.

The battery is the primary ESS, and the supercapacitor is the auxiliary ESS which is connected to a bidirectional DC/DC converter in series and then connected to the battery in parallel. This configuration is beneficial for increasing the DC/DC converter’s energy conversion efficiency and the system controllability due to the rapid response of the supercapacitor voltage. The battery and the supercapacitor cover the smooth and the frequent transient loads respectively during the propulsion mode of the vehicle, and in a similar way, they are responsible for the smooth charging and the frequent charging respectively during regenerative braking mode of the vehicle. In some cases, it is possible for the supercapacitor to be charged by the battery.

2.1 Vehicle Dynamics

BMW i3 EV is selected as the target vehicle in this research, parameters of which are listed in Table 1 [26]. Usually, the vehicle dynamics during driving can be expressed as follows:

$$\begin{aligned}
 F_t - F_r - F_a - F_g &= m \cdot a \\
 F_t - f_r mg \cos \alpha - 0.5 \rho_a A_f C_D v^2 - mg \sin \alpha &= m \cdot a
 \end{aligned}
 \tag{1}$$

where F_t is the traction force provided by the vehicle power system, and F_r , F_a , and F_g represent the tire rolling

resistance, the aerodynamic drag, and the uphill resistance respectively. m is the vehicle total mass, and a is the vehicle acceleration.

Equation (1) is widely adopted in the vehicle energy management research previously. However, this equation is not always appropriate because sometimes results derived from it can be much different from the real case especially the tire rolling resistance and the aerodynamic drag. In order to figure out this problem, the sum of the tire rolling resistance and the aerodynamic drag during driving F_{f+w} is expressed using the vehicle speed v and three coefficients as follows:

$$F_{f+w} = A + Bv + Cv^2 \tag{2}$$

where coefficients A , B , and C are fitted by the real vehicle coast-down experiments [27]. Argonne National Laboratory has conducted the experiments and provided those coefficients for a number of EV models including the BMW i3 [28]. According to the provided data, Eq. (2) for the BMW i3 is fixed as follows:

$$F_{f+w} = 104.907 + 1.8321v + 0.026498v^2 \tag{3}$$

and accordingly, the Eq. (1) can be revised as follows:

$$F_t - (104.907 + 1.8321v + 0.026498v^2) - mg \sin \alpha = m \cdot a \tag{4}$$

where α represents the road slope. Equation (4) is used to express the vehicle dynamics in this research.

2.2 Motor Model

The electric motor is one of the most important components for EVs, which transfers the electrical energy of the HESS into the mechanical energy to propel the vehicle during the propulsion mode. Oppositely, the motor is controlled to be

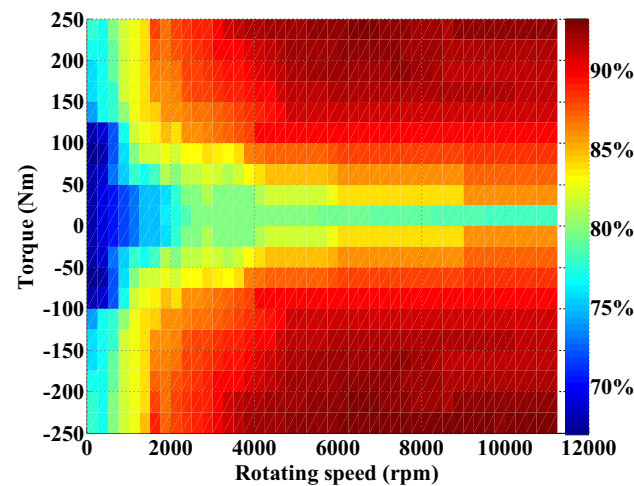


Fig. 2 Motor efficiency map of the BMW i3

working as a generator and transfers the mechanical energy of the vehicle into the electrical energy and stores it into the HESS during the regenerative braking mode. The motor is usually modeled by a motor efficiency map, which expresses the relationship among the speed, the torque, and the efficiency. According to the open data of the BMW i3 [29], the motor efficiency map can be derived as shown in Fig. 2, where quadrants I and IV correspond to the propulsion mode and the regenerative braking mode respectively. Some important parameters of the motor are listed in Table 2.

2.3 Battery Model

The internal resistance model is used for the battery, in which the battery is expressed by a voltage source and a resistance connected to the voltage source in series. The voltage source and the resistance change according to the battery state of charge (SOC). The equivalent circuit diagram of the battery model is illustrated in Fig. 3, in which U_{oc} and R_{int} represent the voltage source, which is called the open circuit voltage (OCV), and the internal resistance respectively.

The following relationship can be drawn from Fig. 3:

$$\begin{aligned} P_b &= U_{bat} \cdot I_{bat} = (U_{oc}(SOC_b) - I_{bat} \cdot R_{int}(SOC_b)) \cdot I_{bat} \\ P_b - (U_{oc}(SOC_b) - I_{bat} \cdot R_{int}(SOC_b)) \cdot I_{bat} &= 0 \end{aligned} \tag{5}$$

where P_b is the battery power and I_{bat} is the battery current. I_{bat} can be expressed as follows by solving the quadratic equation in (5).

$$I_{bat} = \frac{U_{oc}(SOC_b) \pm \sqrt{U_{oc}(SOC_b)^2 - 4R_{int}(SOC_b) \cdot P_b}}{2R_{int}(SOC_b)} \tag{6}$$

Table 2 Parameters of the motor

Parameter	Value
Max power (kW)	125
Max speed (rpm)	11,400
Max torque (Nm)	250

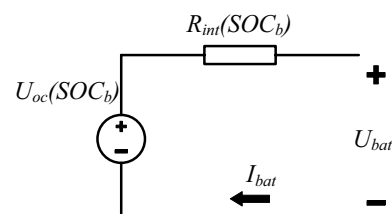


Fig. 3 Equivalent circuit diagram of the battery model

For a certain battery power, there are two different operating modes, i.e. the high-current low-voltage mode and the opposite mode. The high current causes the battery performance degradation including its lifetime, thus it is not suitable for the battery operation. The low-current high-voltage mode is usually preferred for the battery modeling, therefore the minus is selected in Eq. (6) as follows:

$$I_{bat} = \frac{U_{oc}(SOC_b) - \sqrt{U_{oc}(SOC_b)^2 - 4R_{int}(SOC_b) \cdot P_b}}{2R_{int}(SOC_b)} \tag{7}$$

The battery SOC is calculated by the ampere-hour integral method as follows:

$$\dot{SOC}_b = -\frac{I_{bat}}{Q} \tag{8}$$

where Q represents the battery capacity, which is assumed to be a constant value here.

2.4 Supercapacitor Model

The equivalent circuit diagram of the supercapacitor used in this research is illustrated in Fig. 4. A resistance R_s is connected to the capacitor in series, which indicates the internal resistance characteristic of the supercapacitor, while the other resistance R_p is connected to the capacitor in parallel to express the overall leakage phenomenon of the supercapacitor.

According to the relationship in Fig. 4, the following equations can be drawn:

$$\begin{aligned} U_{cap} &= U_c - I_{cap}R_s \\ P_s &= U_{cap} \cdot I_{cap} \\ I_c &= \frac{dU_c}{dt} = \begin{cases} -\frac{1}{C_p R_p} U_c + \frac{I_{cap}}{C_p} & I_{cap} \geq 0 \\ \frac{1}{C_p R_p} U_c + \frac{I_{cap}}{C_p} & I_{cap} \leq 0 \end{cases} \end{aligned} \tag{9}$$

where C_p represents the capacitance of the supercapacitor and P_s is the supercapacitor output power. The supercapacitor SOC is calculated in the same way as the battery, as follows:

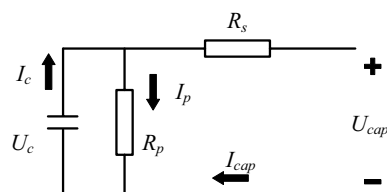


Fig. 4 Equivalent circuit diagram of the supercapacitor model

$$\begin{aligned} S \dot{O} C_s &= -\frac{1}{C_p} \cdot \left[\left(\frac{1}{2R_s} \pm \frac{1}{R_p} \right) \cdot SOC_s \right. \\ &\quad \left. - \frac{1}{2R_s} \sqrt{SOC_s^2 - \frac{4R_s}{V_{c,max}^2} \cdot P_s} \right] \end{aligned} \tag{10}$$

where $V_{c,max}$ is the maximum capacitance voltage. The plus corresponds to the discharging case, whereas the minus corresponds to the charging case.

2.5 Bidirectional DC/DC Converter Model

The bidirectional DC/DC converter in the HESS can be regarded as a voltage regulator on the supercapacitor side, which controls the power distribution between the battery and the supercapacitor. A number of power electronic devices form the bridge buck-boost converter, and it is possible for it to realize the bidirectional energy flow either from the high voltage side to the low voltage side and vice versa. In this research, the bidirectional DC/DC converter is modeled by using an efficiency map as illustrated in Fig. 5, which provides the relationship among the converter efficiency, the supercapacitor output power, and the voltage transformer ratio of the converter.

2.6 HESS Design

The supercapacitor and the DC/DC converter should be newly designed on the basis of the battery to form the HESS. Data of the BMW i3 battery produced by Samsung SDI are listed in Table 3. The battery internal resistance information can be consulted in the literature [30].

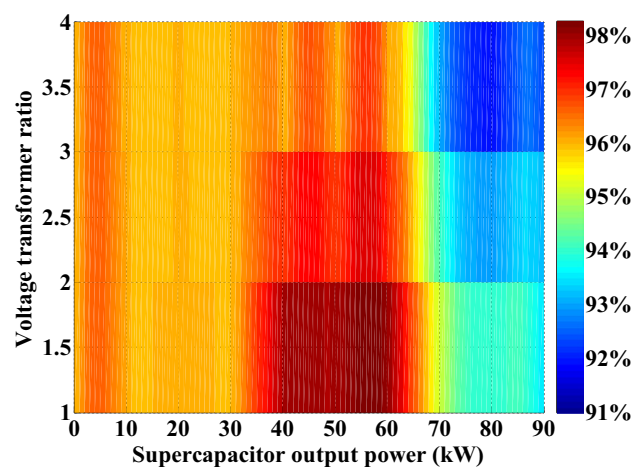


Fig. 5 Efficiency map of the DC/DC converter

2.6.1 Supercapacitor Sizing

The most significant factor for the supercapacitor sizing is the driving condition of the vehicle, as the role of the supercapacitor is to meet the peak power demands during driving. In this research, the supercapacitor is selected to be able to cover all the high power parts during driving, which is above the average required power of the vehicle. Because the energy capacity of the supercapacitor is very low and it can be charged rapidly during deceleration after discharging during acceleration in a city driving condition, considering one extreme driving case in the whole driving cycle is sufficient for the supercapacitor sizing. Additionally, the following relationship is adopted in order to protect the supercapacitor.

$$E_s = E_{cycle_extreme}/0.75 \tag{11}$$

where E_s is the finally selected supercapacitor energy, and $E_{cycle_extreme}$ is the one calculated from the driving cycle for the most extreme case. Considering several typical driving cycles, the following supercapacitor produced by Maxwell is selected as shown in Table 4.

2.6.2 Bidirectional DC/DC Converter Sizing

The selection of the DC/DC converter also depends on the driving condition of the vehicle, especially the peak power demand during the propelling mode and the peak regenerative braking power, and the size of the supercapacitor. Considering several typical driving cycles and the supercapacitor selected in 2.6.1, the DC/DC converter is chosen as shown in Table 5, which is produced by a local supplier. The efficiency map of the selected converter is illustrated in Fig. 6.

The increased mass and volume caused by the supercapacitor and the DC/DC converter is about 60 kg and 50 L respectively in this research, which can be ignored.

3 An EMS Design for the HESS

An EMS is a significant factor for the HESS, which adequately distributes the totally required power between the two ESSs, so that the superiority of each ESS can be

Table 4 Parameters of the selected supercapacitor (Maxwell DuraBlue series)

Parameter	Symbol in equations	Value
Cell model		BCAP3400 P285
Energy capacity (Wh)	E_s	350
Cell number and connection		94 in series
Capacitance (F)	C_p	37
Series resistance (Ω)	R_s	0.027
Parallel resistance (Ω)	R_p	15,272
Maximum capacitance voltage (V)	$V_{c,max}$	262

achieved. In addition, the EMS can also protect each ESS by limiting the over-charging and the over-discharging. A driving condition-adaptive rule-based EMS is proposed in this research which considers the superiority achievement of each ESS and the protection to each ESS at the same time. There are several control parameters defined in the EMS, which are dependent on the driving cycle. The EMS is established based on the driving condition and the status of the vehicle for both the driving mode and the regenerative mode, and in each mode, several operating modes of the HESS are defined.

Figure 6 illustrates the control flowchart of the rule-based EMS proposed in this research. The supercapacitor involving power P_{in} and P_{-in} and the battery constant power $P_{b_constant}$ are all the driving cycle-dependent parameters. P_{in} and P_{-in} are threshold values of the required power of the vehicle P_{req} , which determine whether the supercapacitor starts to work in the vehicle propelling and regenerative modes respectively. $P_{b_constant}$ is the battery power output during the supercapacitor charging mode for the vehicle propelling mode.

Several threshold values are set in the EMS including the supercapacitor involving power P_{in} and P_{-in} , which are defined as the average totally required power of the vehicle for the propelling and regenerative modes respectively, the supercapacitor target SOC SOC_{s_target} , the setting objective of which is to maintain the supercapacitor SOC in the desired range so that the supercapacitor is ready to be charged or discharged anytime, the upper and lower limits of the supercapacitor SOC SOC_{s_max} and

Table 3 Parameters of BMW i3 battery (2018 version)

Parameter	Value
Cell type	NCM
Cell number and connection	96 in series
Rated voltage (V)	355
Capacity (Ah)	120

Table 5 Parameters of the selected DC/DC converter

Parameter	Value
Circuit type	Half H-bridge
Rated power (kW)	35
High voltage side range (V)	250–400
Low voltage side range (V)	100–300

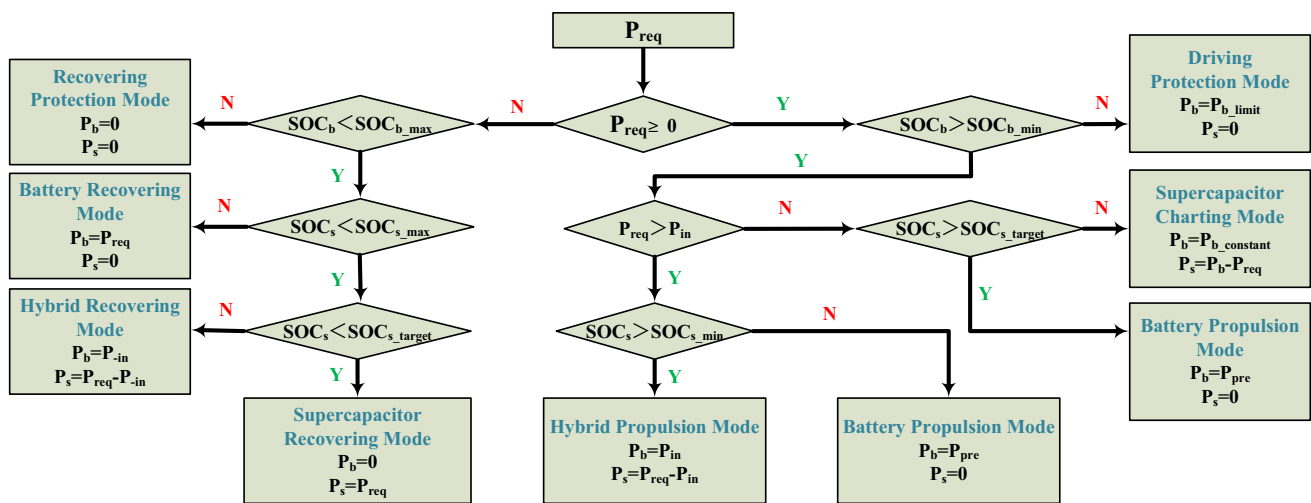


Fig. 6 Control flow chart of the proposed EMS

SOC_{s_min} , the upper and lower limits of the battery SOC SOC_{b_max} and SOC_{b_min} , the lower limit of the battery power P_{b_limit} , which is set to protect the battery during the vehicle propelling mode.

Besides the power distribution rules, the following rules are also adopted in the proposed EMS from the HESS protection point of view:

- In the driving mode, if the battery SOC is less than its lower limit SOC_{b_min} , in order to protect the battery and keep the vehicle’s driving, the battery output power will be limited to P_{b_limit} and the supercapacitor will not work anymore, which corresponds to the driving protection mode in Fig. 6;

- In the regenerative mode, if the battery SOC is greater than its upper limit SOC_{b_max} , the regeneration mode will be terminated, which corresponds to the recovering protection mode in Fig. 6.

4 Validation of the HESS plus EMS

Regarding the effectiveness validation of the HESS plus the EMS, the computer simulation is the most commonly used means owing to the time-saving and cost-saving characteristics. However, the reliability of the computer simulation validation is comparatively low due to the ideal simulation environment. The real vehicle test validation [10, 31] is the closest means to the reality, but it is cost-consuming and some safety problems may occur. Thus, some researchers have concentrated on the semi-physical validation, which can be divided into the RCP [24, 32, 33] and the hardware in the loop (HIL) [34]. In the former, the control objects, such as the battery, the supercapacitor, and the DC/DC converter, are real and the controller is virtual, which is constructed in

the computer simulation program, whereas in the latter, it is the opposite. For a real vehicle development process, the RCP validation is the previous step to the HIL validation.

The effectiveness of the HESS plus the EMS is validated in this section by both the computer simulation and the RCP test. In order to emphasize the superiority of the HESS in EV applications, the validation results of the HESS are compared to those of the single battery case. Three representative driving cycles are selected for the validation in this research as shown in Figs. 7 and 8, which are the China Automotive Test Cycle (CATC), New European Driving Cycle (NEDC), and Urban Dynamometer Driving Schedule (UDDS) respectively. Among them, the CATC is the representative China automotive test cycle, which will be issued soon [35].

4.1 Computer Simulation Validation

Each component of the EV is modeled by the computer simulation program based on Sect. 2, and the management algorithm is also established in the computer simulation environment based on Sect. 3. The threshold values defined in the EMS are set based on experience and simulation tests as listed in Table 6.

4.1.1 Simulation Results of the Proposed EMS

Figures 9, 10, and 11 illustrate the simulation results of the proposed EMS on the CATC, NEDC, and UDDS respectively. The results show that the supercapacitor responds to the frequent power transient requirements and the peak power demands of the vehicle so that the working status of the battery is stabilized during the propelling mode. During the regeneration mode, the supercapacitor recovers most of

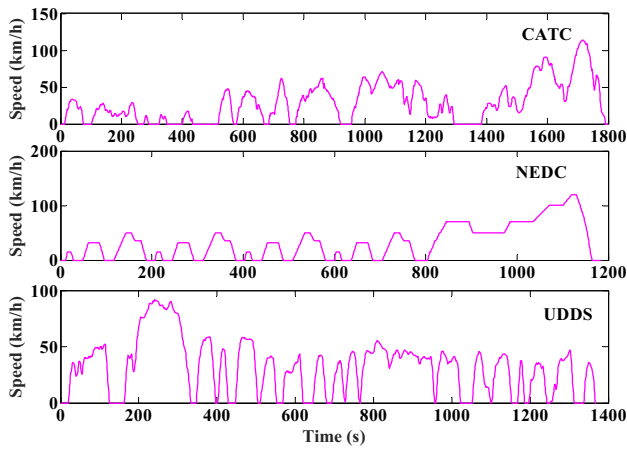


Fig. 7 Three representative driving cycles used in this research

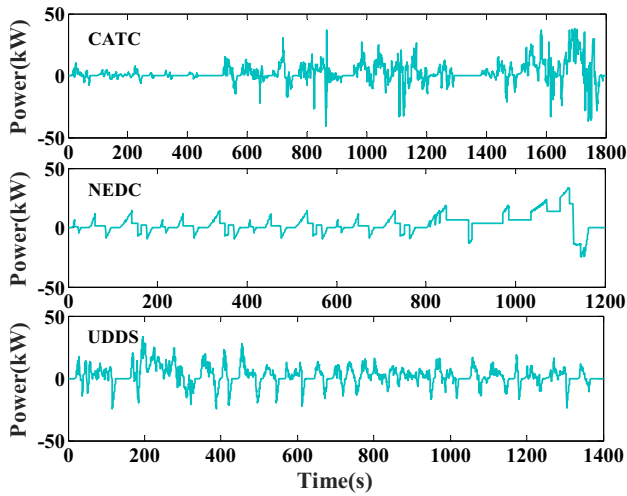


Fig. 8 Required power for the vehicle on the three representative driving cycles

Table 6 Threshold values defined in the EMS

Parameter	Value
Supercapacitor target SOC SOC_{s_target}	0.8
Upper limit of supercapacitor SOC_{s_max}	0.99
Lower limit of supercapacitor SOC_{s_min}	0.5
Upper limit of battery SOC_{b_max}	0.95
Lower limit of battery SOC_{b_min}	0.2

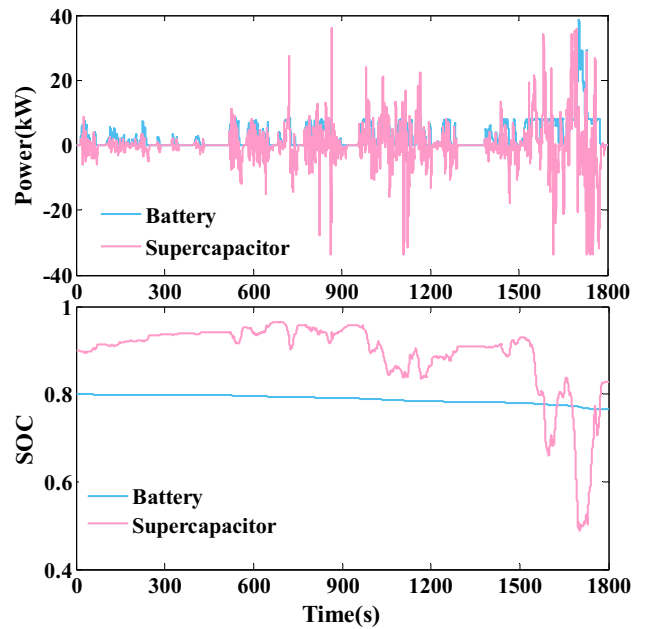


Fig. 9 Simulation results of the proposed EMS on the CATC

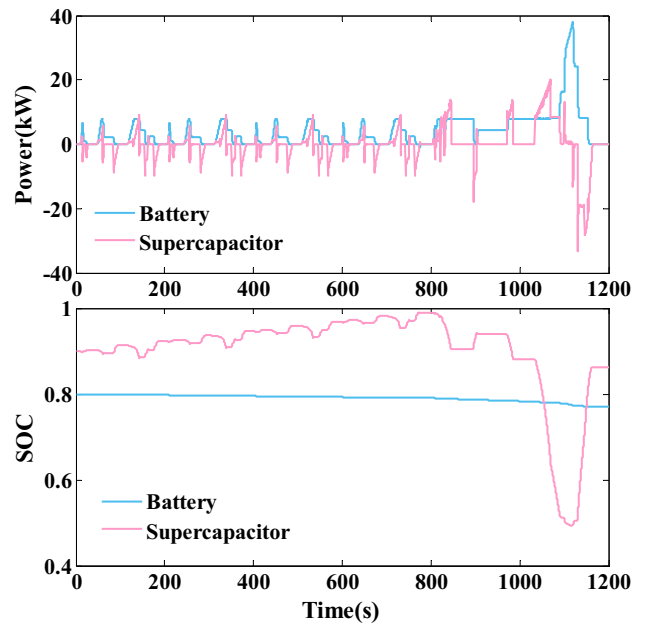


Fig. 10 Simulation results of the proposed EMS on the NEDC

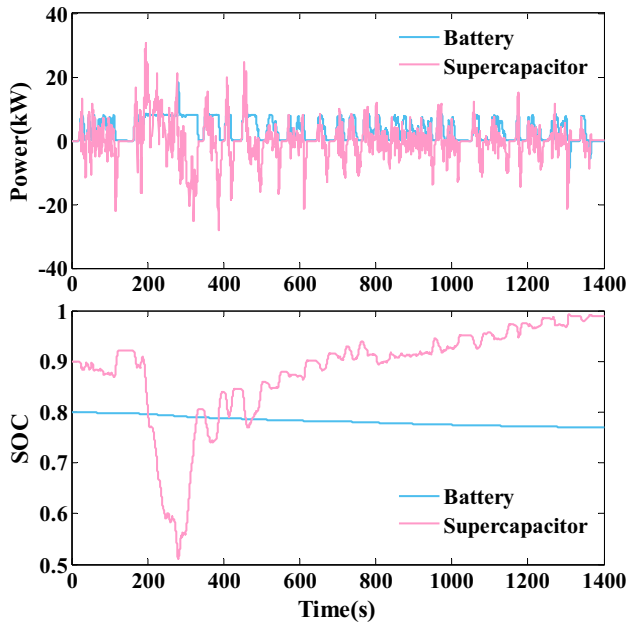


Fig. 11 Simulation results of the proposed EMS on the UDSS

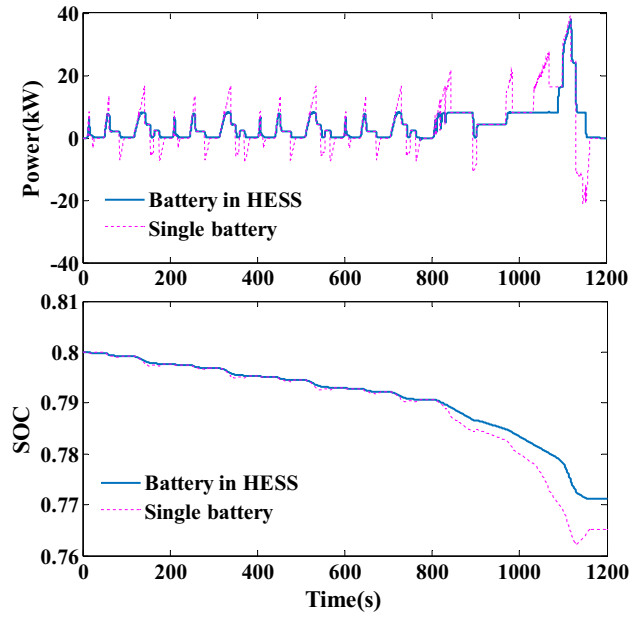


Fig. 13 Simulation results comparison between the HESS and the single battery cases on the NEDC

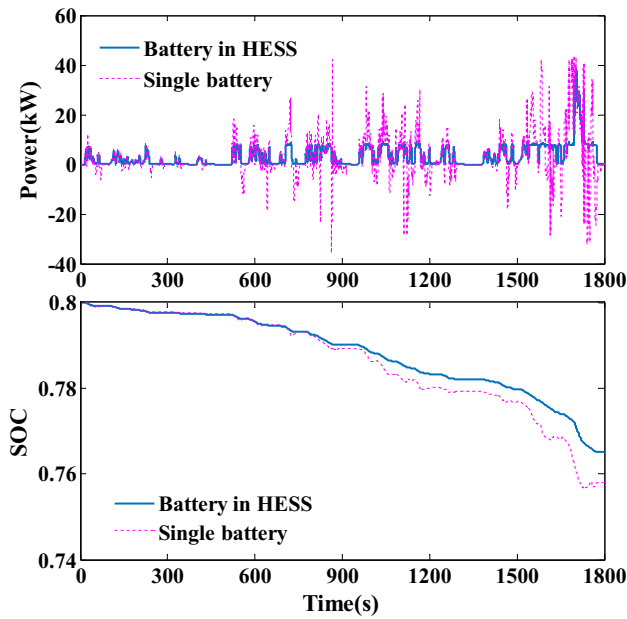


Fig. 12 Simulation results comparison between the HESS and the single battery cases on the CATC

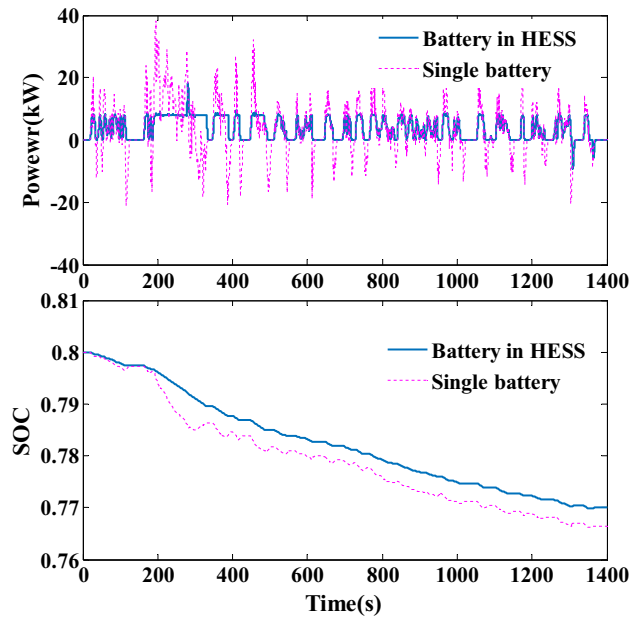


Fig. 14 Simulation results comparison between the HESS and the single battery cases on the UDSS

Table 7 Average changing rate comparison of battery output power

Driving cycle	HES case (kW/s)	Single battery case (kW/s)	Decrease percentage (%)
CATC	0.68	2.90	76.5
NEDC	0.27	0.77	64.9
UDDS	0.65	2.54	74.4

Table 8 Average battery current comparison

Driving cycle	HES case (A)	Single battery case (A)	Reducing percentage (%)
CATC (propelling)	9.49	21.50	55.9
NEDC (propelling)	10.89	21.24	48.7
UDDS (propelling)	10.25	20.75	50.6
CATC (regeneration)	0	−10.23	100
NEDC (regeneration)	−0.18	−14.91	98.8
UDDS (regeneration)	−2.37	−13.34	82.2

the regenerative braking energy so that the battery is relieved from the frequent working mode changes between the charging and discharging.

4.1.2 Simulation Comparison to the Single Battery Case

Figures 12, 13, and 14 show the comparison results between the HES case and the single battery case on the CATC, NEDC, and UDDS respectively. The battery is the same for the two cases, and the small difference in the total vehicle mass between the two cases is neglected. It can be observed from the comparison results that the trajectories of the battery output power and the battery SOC are smoother for the HES case compared to the single battery case, which is beneficial for prolonging the battery lifetime. The battery undertakes the energy shocks alone during both the propelling and regenerative modes in the single battery case, which will definitely shorten its lifetime, whereas this problem can be eliminated in the HES case.

Table 7 provides the simulation results on the average changing rate of the battery output power for both the HES case and the single battery case, which indicates that a maximum of 76.5% decrease on the average output power changing rate of the battery can be achieved by the use of the HES. This decrease will result in prolonging the battery lifetime.

Table 9 Final battery SOC comparison

Driving cycle	HES case	Single battery case	Decrease percentage (%)
CATC	0.69	0.67	2.8
NEDC	0.71	0.69	2.4
UDDS	0.71	0.70	1.9

Table 10 Q_{loss_cycle} for each case (10^{-4} %)

	CATC	NEDC	UDDS
HES	6.25	7.77	7.77
Single battery	10.07	10.57	9.46

Table 8 presents the simulation results comparison on the average battery current for both the propelling and the regeneration modes. It reveals that the average battery current is reduced dramatically, for some case even reduced to 0, by the use of the HES compared to the single battery case for both the propelling and the regeneration modes. This will also result in prolonging the battery lifetime [9].

The battery energy is also saved in the HES case compared to the single battery case because of the improvement on the battery efficiency. The final battery SOC after three times of repetitions for each driving cycle is summarized in Table 9, which reveals that a maximum of 2.8% of the battery energy can be saved by the use of the HES.

4.1.3 Life Cycle Cost Analysis of HES

Comparison results in 4.1.2 show that the HES is good for prolonging the battery lifetime and also beneficial for saving the battery energy. However, the addition of the supercapacitor and the DC/DC converter will also increase the system cost, thus an economic analysis is necessary for the life cycle cost comparison between the HES and the single battery cases.

A dynamic degradation model [3] for the battery is adopted to evaluate the battery capacity loss during driving, as follows:

$$Q_{loss} = Ae^{-\left(\frac{E_a + B \cdot C_{Rate}}{R \cdot T_{bat}}\right)} (A_h)^z \quad (12)$$

where Q_{loss} represents the battery capacity loss in percentage, A is the pre-exponential factor, E_a is the activation energy (J), R is the gas constant (J/(mol K)), T_{bat} is the absolute temperature (K), A_h is the Ah-throughput, C_{Rate} is the battery discharging rate, and B is the compensation factor of

Table 11 $cost_{life_cycle}$ for each case (10^{-2}¥/km)

	CATC	NEDC	UDDS
HESS	10.33	16.89	15.48
Single battery	15.02	20.76	17.03

C_Rate . Assuming that the battery should be replaced when its capacity decreases to 80% of the original status, then the life cycle cost of the HESS and the single battery for each driving cycle can be obtained as follows:

$$cost_{life_cycle} = \frac{cost_{bat} + cost_{sup} + cost_{DC/DC}}{D_{cycle} \cdot (20/Q_{loss_cycle})} \quad (13)$$

where $cost_{bat}$, $cost_{sup}$, and $cost_{DC/DC}$ represent the cost of the battery, the supercapacitor, and the DC/DC converter, respectively, D_{cycle} is the driving distance of each driving cycle, Q_{loss_cycle} is the battery capacity loss corresponding to one accomplishment of each driving cycle derived from (12), which is listed in Table 10 for each case. The battery lifetime prolonging effect benefited from the HESS is quantitatively proved in Table 10. Considering the Chinese market, 1000¥/kWh for the battery, 10,000¥/kWh for the supercapacitor, and 30¥/kW for the DC/DC converter are adopted for the costs of each component, and the life cycle cost $cost_{life_cycle}$ for each case derived from (13) is listed in Table 11. It can be concluded from Table 11 that although

the addition of the supercapacitor and the DC/DC converter increases the initial cost of the system, the life cycle cost of the HESS is lower than that of the single battery owing to the battery lifetime prolonging effect.

4.2 RCP Validation

The computer simulation environment is very ideal compared to reality, in which there are no communication delays between components and a number of assumptions applied to each component. In order to validate the HESS plus the EMS in a more realistic environment, the RCP validation is adopted in this research, in which the control objectives, such as the battery, the supercapacitor, and the DC/DC converter, are the real components while the controller is virtual, which is established in the simulation program. The schematic diagram of the test bench is illustrated in Fig. 15, in which the dSPACE Microlabbox is used in the connection between the hardware and the software. An electric loading equipment is used to simulate the totally required power according to the driving cycle. The Microlabbox receives signals from current sensors, which are equipped in the bus, the battery, and the supercapacitor, and the electric loading equipment and controls the bidirectional DC/DC converter based on the EMS and the received signals, so that the rule-based EMS is realized to the real powertrain components.

Figure 16 shows the test bench, in which the real components are downsized compared to the original ones introduced in Sect. 2 considering the safety and cost of the experiment. The DC bus voltage, the current, and the electric loading levels are accordingly downsized to 1/3, 1/8, and 1/24 respectively. Additionally, a filter function is applied to the battery current in order to reduce the impact of sudden currents to the battery. The information on each component of the test bench is shown in Table 12.

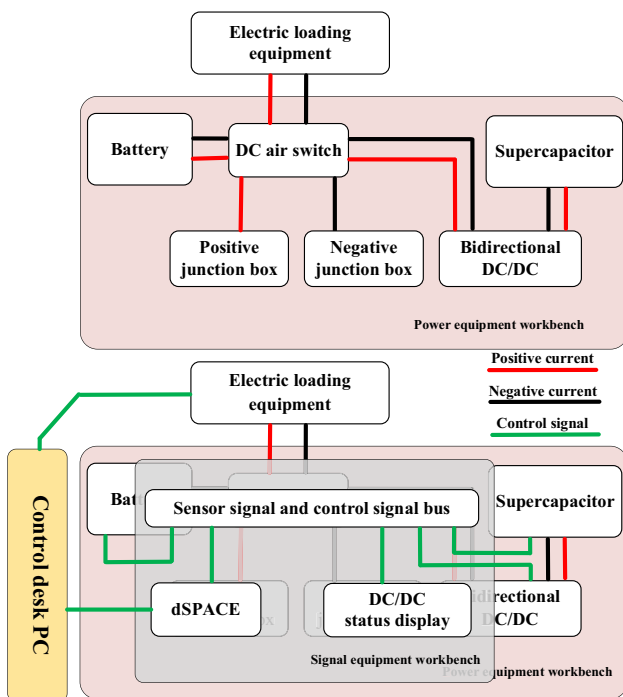


Fig. 15 Schematic diagram of the test bench

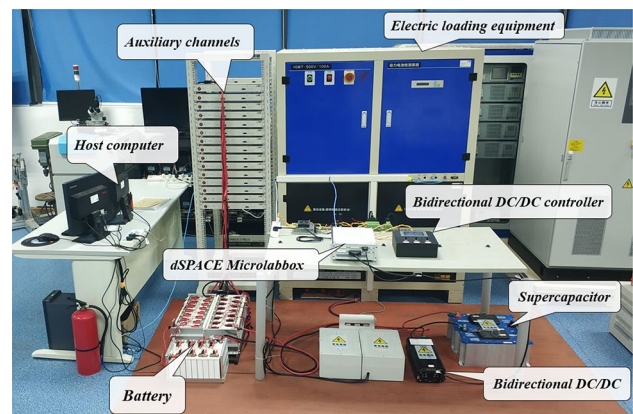


Fig. 16 Test bench for the RCP validation

Table 12 Information on each component of the test bench






Component	Parameters	Photo
dSPACE Microlabbox	Model: RTI1202; Communication: CAN/Serial	
Electric loading equipment	Voltage: 0~822 V; Current: -200A~200A; Sampling frequency: 100 Hz; Response time: ≤20mS	
Battery	Type: Lithium iron phosphate Connection: 39 cells in series; Voltage: 110 V~140 V; Capacity: 5kWh	
Supercapacitor	Model: Maxwell; Connection: 2cells in series; Voltage: 48 V~95 V; Capacity: 82.5F	
Bidirectional DC/DC	Voltage: 40 V~250 V; Current: -30A~30A; Rated power: 3 kW	

Fig. 17 Test results of the proposed EMS on the CATC

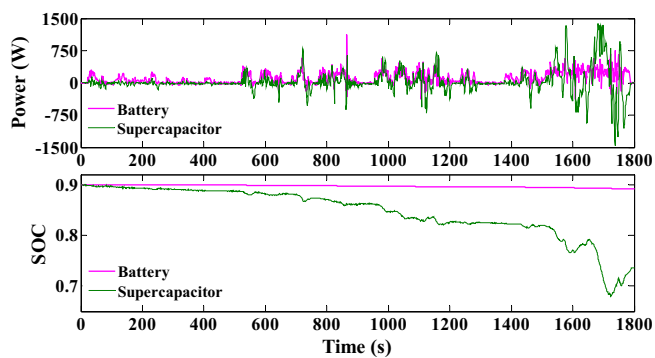


Fig. 18 Test results of the proposed EMS on the NEDC

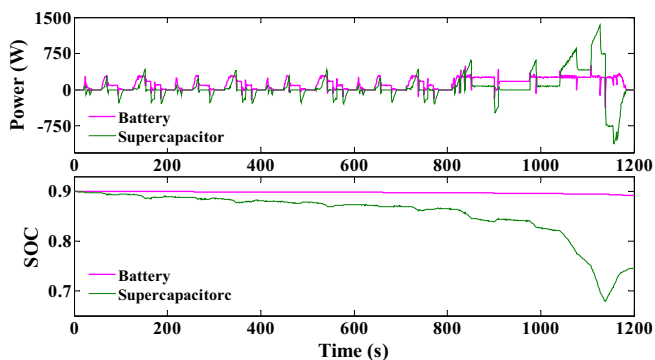


Fig. 19 Test results of the proposed EMS on the UDDS

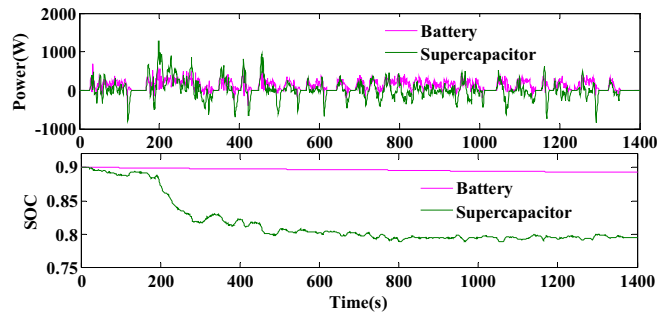


Fig. 20 Battery test results comparison on the CATC

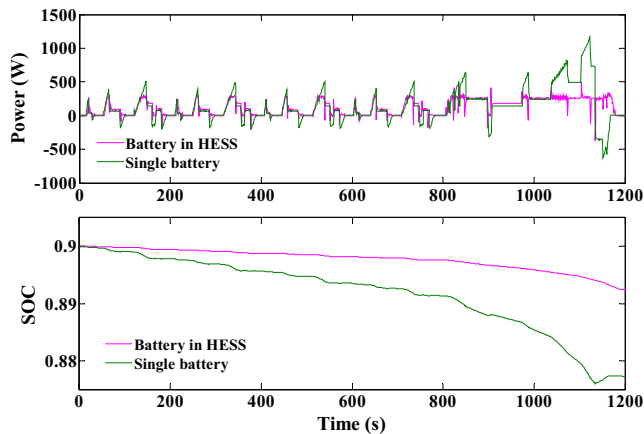
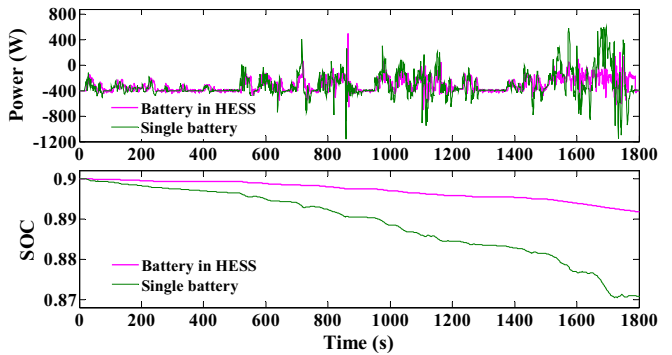
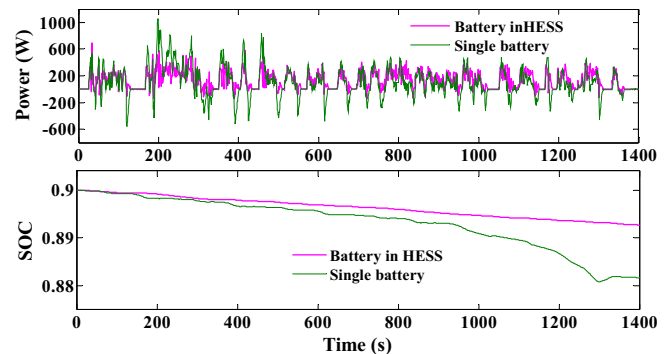


Fig. 21 Battery test results comparison on the NEDC

Fig. 22 Battery test results comparison on the UDDS



4.2.1 Test Results of the Proposed EMS

Figures 17, 18, and 19 illustrate the test results on the three driving cycles respectively. The tendency of the test results is consistent with that of the simulation results, in which both the energy density superiority of the battery and the power density superiority of the supercapacitor are achieved. The communication delays between components and the response delay of the DC/DC converter influence the test results. Besides, there are usually noisy signals in the communication system caused by the thermal effect or unwanted

Table 13 Final battery SOC comparison

Driving cycle	HES case	Single battery case	Decrease percentage (%)
CATC	0.891	0.871	2.3
NEDC	0.892	0.877	1.7
UDDS	0.892	0.882	1.1

external disturbing. These are the main reasons for the image difference between the computer simulation and the test results.

4.2.2 Test Comparison to the Single Battery Case

Figures 20, 21, and 22 show the test results comparison between the HESS case and the single battery case on the three driving cycles respectively, in which the battery lifetime prolonging effect and the battery energy saving effect of the HESS under the EMS can both be checked. Table 13 shows the final battery SOC for each case for the three driving cycles, which indicates that a maximum of 2.3% of the battery energy can be saved by the use of the HESS. Table 14 provides the battery capacity loss Q_{loss_cycle} obtained from (12) and the life cycle cost $cost_{life_cycle}$ obtained from (13) for each case, which also indicates that the life cycle cost of the HESS is lower than that of the single battery due to its battery lifetime prolonging effect. The values are much less than those in Tables 10 and 11 due to the relatively small battery current in the test.

5 Conclusion

The effectiveness of the HESS in a commercialized EV model is validated in this research. The HESS is designed for the BMW i3 and the driving condition-adaptive rule-based EMS is proposed for the HESS because it is simple

and convenient for both the establishment and the validation compared to other types of EMSs. The HESS plus the EMS is validated by both the computer simulation and the RCP semi-physical test. Both validations show the following results:

- (1) Compared to the single battery case, the trajectories of the battery output power and the battery SOC are smoother in the HESS case. Simulation results indicate that a maximum of 76.5% decrease on the average output power changing rate of the battery can be achieved by the use of the HESS and dramatic decreases on the average battery current can also be realized by the use of the HESS for both the propelling mode and the regeneration mode. The battery lifetime prolonging effect benefited from the HESS is quantitatively proved by comparing the battery capacity loss for the HESS and the single battery cases based on the battery dynamic degradation model.
- (2) The battery energy is also saved in the HESS case compared to the single battery case. According to the simulation results, a maximum of 2.8% of the battery energy is saved by the use of the HESS.
- (3) Although the addition of the supercapacitor and the DC/DC converter increases the initial cost of the system, the life cycle cost of the HESS is lower than that of the single battery owing to the battery lifetime prolonging effect, thus the HESS is economically effective.
- (4) The tendency of the RCP test results is consistent with that of the simulation results. The communication delays between components and the response delay of the DC/DC converter are the main reasons for the image difference between both results. The battery energy saving effect and the economic effectiveness of the HESS are proved similarly based on the RCP test results.

Future work of this research is to reduce the number of assumptions used in the simulation models and remedy the limitations of this research for example adopting flexible threshold values for the EMS in order to increase the adaptability.

Table 14 Q_{loss_cycle} (10^{-4} %) and $cost_{life_cycle}$ (10^{-2} ¥/km) for each case

	CATC		NEDC		UDDS	
	HES case	Single battery	HES case	Single battery	HES case	Single battery
Q_{loss_cycle}	0.462	0.750	0.356	0.587	0.367	0.599
$cost_{life_cycle}$	0.76	1.12	0.78	1.16	0.73	1.08

Acknowledgement This research was supported by Shenzhen Science and Technology Innovation Commission (Grant Nos. KQJSCX20180330170047681 and JCYJ20180507182628567), National Key Research and Development Program of China (Grant No. 2016YFD0700602), National Natural Science Foundation of China (NSFC) (51707191), Chinese Academy of Sciences PIFI program (2021VEB0001), and Shenzhen Key Laboratory of Electric Vehicle Powertrain Platform and Safety Technology.

References

- Armenta, J., Núñez, C., Visairo, N., & Lázaro, I. (2015). An advanced energy management system for controlling the ultracapacitor discharge and improving the electric vehicle range. *Journal of Power Sources*, 284, 452–458.
- Carter, R., Cruden, A., & Hall, P. J. (2012). Optimizing for efficiency or battery life in a battery/supercapacitor electric vehicle. *IEEE Transactions on Vehicular Technology*, 61(4), 1526–1533.
- Song, Z., Hofmann, H., Li, J., Hou, J., Han, X., & Ouyang, M. (2014). Energy management strategies comparison for electric vehicles with hybrid energy storage system. *Applied Energy*, 134, 321–331.
- Zhang, Q., Deng, W., Zhang, S., & Wu, J. (2016). A rule based energy management system of experimental battery/supercapacitor hybrid energy storage system for electric vehicles. *Journal of Control Science and Engineering*, 2016, 1–17.
- Li, Y., Huang, X., Liu, D., Wang, M., & Xu, J. (2019). Hybrid energy storage system and energy distribution strategy for four-wheel independent-drive electric vehicles. *Journal of Cleaner Production*, 220, 756–770.
- Li, J., Fu, Z., & Jin, X. (2017). Rule based energy management strategy for a battery/ultra-capacitor hybrid energy storage system optimized by pseudo spectral method. *Energy Procedia*, 105, 2705–2711.
- Yan, M., Li, M., He, H., Peng, J., & Sun, C. (2018). Rule-based energy management for dual-source electric buses extracted by wavelet transform. *Journal of Cleaner Production*, 189, 116–127.
- Florescu, A., Bacha, S., Munteanu, L., Bratcu, A. L., & Rumeau, A. (2015). Adaptive frequency-separation-based energy management system for electric vehicles. *Journal of Power Sources*, 280, 410–421.
- Zheng, C., Li, W., & Liang, Q. (2018). An energy management strategy of hybrid energy storage systems for electric vehicle applications. *IEEE Transactions on Sustainable Energy*, 9(4), 1880–1888.
- Long, B., Lim, S. T., Bai, Z. F., Ryu, J. H., & Chong, K. T. (2014). Energy management and control of electric vehicles, using hybrid power source in regenerative braking operation. *Energies*, 7(7), 4300–4315.
- Santucci, A., Sorniotti, A., & Lekakou, C. (2014). Power split strategies for hybrid energy storage systems for vehicular applications. *Journal of Power Sources*, 258, 395–407.
- Kim, N., Jeong, J., & Zheng, C. (2019). Adaptive energy management strategy for plug-in hybrid electric vehicles with Pontryagin's minimum principle based on daily driving patterns. *International Journal of Precision Engineering and Manufacturing-Green Technology*, 6(3), 539–548.
- Zheng, C., & Cha, S. W. (2017). Real-time application of Pontryagin's minimum principle to fuel cell hybrid buses based on driving characteristics of buses. *International Journal of Precision Engineering and Manufacturing-Green Technology*, 4(2), 199–209.
- Song, Z. Y., Hofmann, H., Li, J. Q., Han, X. B., & Ouyang, M. G. (2015). Optimization for a hybrid energy storage system in electric vehicles using dynamic programming approach. *Applied Energy*, 139, 151–162.
- Wang, B., Xu, J., Cao, B., & Ning, B. (2017). Adaptive mode switch strategy based on simulated annealing optimization of a multi-mode hybrid energy storage system for electric vehicles. *Applied Energy*, 194, 596–608.
- Trovão, J. P., & Antunes, C. H. (2015). A comparative analysis of meta-heuristic methods for power management of a dual energy storage system for electric vehicles. *Energy Conversion and Management*, 95, 281–296.
- Eckert, J. J., de Alkmin e Silva, L. C., Santiciolli, F. M., dos Santos Costa, E., Corrêa, F. C., & Dedini, F. C. (2018). Energy storage and control optimization for an electric vehicle. *International Journal of Energy Research*, 42, 3506–3523.
- Wang, Bin, Jun, Xu, Cao, Binggang, & Zhou, Xuan. (2015). A novel multimode hybrid energy storage system and its energy management strategy for electric vehicles. *Journal of Power Sources*, 281, 432–443.
- Trovão, J. P. F., Santos, V. D. N., Pereirinha, P. G., Jorge, H. M., & Antunes, C. H. (2013). A simulated annealing approach for optimal power source management in a small EV. *IEEE Transactions on Sustainable Energy*, 4(4), 867–876.
- Trovão, J. P. F., Santos, V. D. N., Antunes, C. H., Pereirinha, P. G., & Jorge, H. M. (2015). A real-time energy management architecture for multisource electric vehicles. *IEEE Transactions on Industrial Electronics*, 62(5), 3223–3233.
- He, H., Xiong, R., Zhao, K., & Liu, Z. (2013). Energy management strategy research on a hybrid power system by hardware-in-loop experiments. *Applied Energy*, 112, 131–1317.
- Xiong, R., Duan, Y., Cao, J., & Quanqing, Y. (2018). Battery and ultracapacitor in-the-loop approach to validate a real-time power management method for an all-climate electric vehicle. *Applied Energy*, 217, 153–165.
- Amjadi, Z., & Williamson, S. S. (2010). Power-electronics-based solutions for plug-in hybrid electric vehicle energy storage and management systems. *IEEE Transactions on Industrial Electronics*, 57(2), 608–616.
- Cao, J., & Emadi, A. (2012). A new battery/ultracapacitor hybrid energy storage system for electric, hybrid, and plug-in hybrid electric vehicles. *IEEE Transactions on Industrial Electronics*, 27(1), 122–132.
- Lukic, S.M., Wirasingha, S.G., Rodriguez, F., Cao, J., Emadi, A. (2006). Power management of an ultracapacitor/battery hybrid energy storage system in an HEV. In *IEEE Vehicle Power and Propulsion Conference*, (Windsor, UK).
- <https://www.bmwusa.com/vehicles/bmw/i3/sedan/pricing-featurs.html>.
- Preda, I., Covaciu, D., Ciolan, G. (2010). Coast down test—theoretical and experimental approach. In *International Automotive Congress*.
- <https://www.anl.gov/es/energy-systems-d3-2014-bmw-i3bev>.
- https://www.energy.gov/sites/prod/files/2017/08/f36/FY16%20EDT%20Annual%20Report_FINAL.pdf.
- Jongryeol, J., Wonbin, L., Namdoo, K., Kevin, S., Aymeric, R. (2017). Control analysis and model Validation for BMW i3 range extender. *SAE Technical Paper* 2017-01-1152.
- Dixon, J., Nakashima, I., Arcos, E. F., & Ortuzar, M. (2010). Electric vehicle using a combination of ultracapacitor and ZEBAR battery. *IEEE Transactions on Industrial Electronic*, 57(3), 943–949.
- Wang, L., Collines, E. G., & Li, H. (2011). Optimal design and real-time control for energy management in electric vehicles. *The IEEE Transactions on Vehicular Technology*, 60(4), 1419–1429.
- Hredzak, B., Agelidis, V. G., & Jang, M. (2014). A model predictive control system for a hybrid battery-ultracapacitor power source. *IEEE Transactions on Industrial Electronic*, 29(3), 1469–1479.

34. Golchoubian, P., & Azad, N. L. (2017). Real-time nonlinear model predictive control of a battery-supercapacitor hybrid energy storage system in electric vehicles. *IEEE Transactions on Vehicular Technology*, 66(11), 9678–9688.
35. <http://www.catarec.org.cn/upload/201808/01/201808011133125858.pdf>

Publisher's Note Springer Nature remains neutral with regard to jurisdictional claims in published maps and institutional affiliations.



Chunhua Zheng received her Ph.D. from Seoul National University in 2012. She is currently working as an associate professor in Shenzhen Institutes of Advanced Technology, Chinese Academy of Sciences, China.



Yafei Wang received his M. S. from Shenyang University of Technology in 2020. He is currently working as a test engineer in JingWei Hirain, Beijing, China.



Zhongxu Liu received his M. S. from Shandong University of Technology in 2019. He is currently working as a power assembly framework engineer in SAIC Motor, Shanghai, China.



Tianfu Sun received his Ph.D. from Sheffield University in 2016. He is currently working as an associate professor in Shenzhen Institutes of Advanced Technology, Chinese Academy of Sciences, China.



Namwook Kim received his Ph.D. from Seoul National University in 2009. He is currently working as an associate professor in the Department of Mechanical Engineering, Hanyang University ERICA Campus at Ansan, South Korea.



Jongryeol Jeong received his Ph.D. from Seoul National University in 2015. He is currently working as a systems analysis engineer in Center for Transportation Research, Energy Systems Division of Argonne National Lab in U.S.A.



Suk Won Cha received his Ph.D. from Stanford University in 2004. He is currently working as a professor in the Department of Mechanical Engineering, Seoul National University, South Korea.